

Modern Physics Letters A **DESY 13-121, DO-TH 13/17, SFB/CPP-13-44, LPN13-041**  
© World Scientific Publishing Company

## DETERMINATION OF $\alpha_s$ AND $m_c$ IN DEEP-INELASTIC SCATTERING

SERGEY ALEKHIN\*

*Deutsches Elektronen-Synchrotron DESY, Platanenallee 6  
Zeuthen, D15738, Germany  
sergey.alekhin@desy.de*

JOHANNES BLÜMLEIN

*Deutsches Elektronen-Synchrotron DESY, Platanenallee 6  
Zeuthen, D15738, Germany  
johannes.bluemlein@desy.de*

SVEN-OLAF MOCH

*II. Institut für Theoretische Physik, Universität Hamburg, Luruper Chaussee 149  
Hamburg, D-22761, Germany  
sven-olaf.moch@desy.de*

Received (Day Month Year)

Revised (Day Month Year)

We describe the determination of the strong coupling constant  $\alpha_s(M_Z^2)$  and of the charm-quark mass  $m_c(m_c)$  in the  $\overline{\text{MS}}$ -scheme, based on the QCD analysis of the unpolarized World deep-inelastic scattering data. At NNLO the values of  $\alpha_s(M_Z^2) = 0.1134 \pm 0.0011(\text{exp})$  and  $m_c(m_c) = 1.24 \pm 0.03(\text{exp})_{-0.02}^{+0.03}(\text{scale})_{-0.07}^{+0.00}(\text{th})$  are obtained and are compared with other determinations, also clarifying discrepancies.

*Keywords:* Strong coupling constant; charm quark mass; parton distributions.

PACS Nos.: 12.38.Qk, 12.38.Bx.

### 1. Introduction

The process of lepton-nucleon deep-inelastic scattering (DIS) is a clean source of basic information about the hadron substructure in terms of the parton model. Moreover, the QCD corrections to the parton model provide the connection of the DIS structure functions with the parameters of the QCD Lagrangian, in particular to the strong coupling  $\alpha_s$  and the heavy-quark masses. The higher order QCD corrections are manifest in the scaling violations of the structure functions w.r.t. the

\*Permanent address: Institute for High Energy Physics, Pobeda 1, Protvino, 142280, Russia

virtual photon momentum transfer  $Q^2$ . This phenomenon was observed shortly after the discovery of the partonic structure of the nucleon and provided one of the first constraints on  $\alpha_s$ . With the dramatic improvement in the accuracy of the lepton-nucleon DIS data and the progress in the theoretical calculations the value of  $\alpha_s$  can in principle be determined with an accuracy of  $O(1\%)$ <sup>a</sup>. The scaling violations, however, are also sensitive to the parton distribution functions (PDFs). Therefore the determination of  $\alpha_s$  has to be performed simultaneously with the nucleon PDFs in global fits. Furthermore, an elaborate theoretical description of the QCD scaling violations is available for the leading-twist terms only. In practice this requires a careful isolation of the higher-twist effects and/or their independent phenomenological parameterization. Another important aspect of DIS phenomenology is related to the  $c$ - and  $b$ -quark contributions. The heavy-quark production cross section is sensitive to the heavy-quark masses. Therefore the DIS data provide a constraint on the  $c$ - and  $b$ -quark masses,  $m_{c,b}$ . The structure functions of the semi-inclusive process with the heavy quark in the final state are particularly useful for this purpose, although the data on inclusive structure functions are competitive with the semi-inclusive ones due to a much better accuracy. A major pitfall arising in the analysis of heavy quark production is related to the account of the higher-order QCD corrections. Due to the two scales appearing in the problem the calculations are quite involved. Therefore the NNLO corrections to the heavy-quark lepto-production are known in partial form only [2] at present. The problem of the high-order corrections is bypassed in the so-called variable-flavor-number (VFN) scheme assuming zero mass for the  $c$ - and  $b$ -quark. In this approximation the available high-order massless DIS Wilson coefficients can be employed for the calculation of the heavy-quark lepto-production rates. As well-known, the VFN approximation is obviously inapplicable at scales  $Q^2 \sim m_{c,b}^2$  and it is commonly supplemented by *modeling* of the Wilson coefficient at low  $Q^2$  in order to arrive in this way at a general-mass VFN (GMVFN) scheme. In the present paper we essentially focus on the determination of  $\alpha_s$  and  $m_c$  based on the fixed-flavor-number (FFN) scheme. Here the mass effects are taken into account on field-theoretic grounds, free of model ambiguities appearing in the so-called GMVFN schemes. Moreover, we employ the massive Wilson coefficients derived using the running-mass definition, which provide improved perturbative stability of the heavy-quark production rate [3].

The paper is organized as follows. In Section 2 we outline the theoretical basis of the analysis and describe the data used. Sections 3 and 4 contain our results on the determination of  $\alpha_s$  and the  $c$ -quark mass, respectively. In Section 5 we compare the FFN and VFN schemes with particular emphasis on the uncertainties in the determination of  $\alpha_s$  and  $m_c$ .

<sup>a</sup>For a recent overview on precision determinations of  $\alpha_s(M_Z^2)$  see [1].

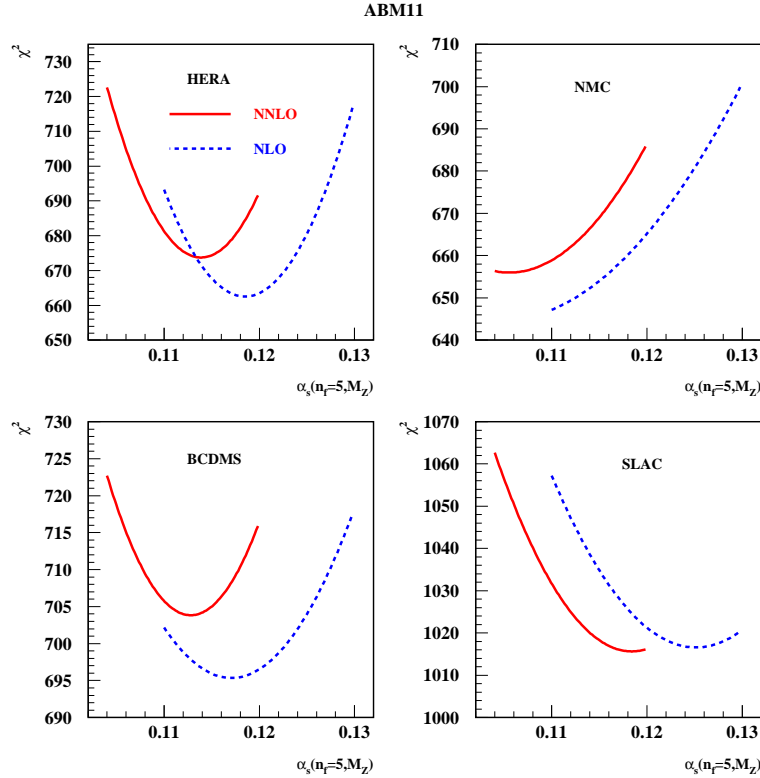


Fig. 1. The  $\chi^2$ -profile versus the value of  $\alpha_s(M_Z^2)$ , for the separate data subsets, all obtained in variants of the ABM11 analysis with the value of  $\alpha_s$  fixed and all other parameters fitted (solid lines: NNLO fit, dashes: NLO fit); from Ref. [4].

## 2. Theoretical and Experimental Ingredients of the Analysis

Our determination of  $\alpha_s$  and  $m_c$  is based on the QCD analysis of the DIS data obtained in fixed-target experiments and at the HERA collider. Only the proton- and deuteron-target samples are selected which allows to minimize the impact of the nuclear corrections on the results<sup>b</sup>. The DIS data are combined with the ones on the fixed-target Drell-Yan process, providing a supplementary constraint on the PDFs and to facilitate the separation of the valence and sea quark distributions. The main version of our analysis is performed at NNLO using the three-loop anomalous dimensions in the PDF evolution and corresponding Wilson coefficients for the light-flavor DIS structure functions and the Drell-Yan process. For the neutral-current (NC) heavy-quark contribution we employ the approximate NNLO Wilson coefficients [2]. These terms were derived combining results obtained with the soft-gluon

<sup>b</sup>For a detailed description of the data set used cf. Ref. [4].

resummation technique and the high-energy limit of the DIS structure functions [5]. These two approaches provide a good approximation at kinematics close to threshold of the heavy-quark production and far beyond the threshold, respectively. Between these two regimes the constraint coming from the available NNLO massive operator-matrix-element (OME) Mellin moments [6] are employed. A remaining uncertainty in the NNLO Wilson coefficient obtained in this way is quantified by its margins, A and B. To find the best shape of the NNLO term preferred by the data we use a linear interpolation between these margins

$$c_2^{(2)} = (1 - d_N)c_2^{(2),A} + d_Nc_2^{(2),B}. \quad (1)$$

and fit the interpolation parameter  $d_N$  to the data simultaneously with the PDF parameters,  $\alpha_s$  and  $m_c$ . The charged-current (CC) heavy-quark production is calculated with account of the NLO corrections [7–9], which are the highest-order ones presently available. Both NC and CC massive Wilson coefficients used in our analysis are used with the  $\overline{\text{MS}}$ -definition of the heavy-quark mass. If compared to the case using the pole-mass the present choice is perturbatively more stable [3]. With the running-mass definition this contribution basically vanishes since the mass can be defined at the typical renormalization/factorization scale of the process considered.

The leading-twist terms provided by the QCD-improved parton model are not sufficient at small  $Q^2$  and/or final-state hadronic mass  $W$ , where parton correlations cannot be neglected. To account for these we add on the top of the leading-twist term the twist-4 contribution to the DIS structure functions  $F_{2,T}$ , parameterized in a model-independent form using spline interpolation<sup>c</sup>. The twist-4 spline coefficients are fitted to the data together with other the parameters. This is particularly important for the case of  $\alpha_s$  in view of its strong correlation with the higher twist terms.

### 3. Strong Coupling Constant

The strong coupling constant  $\alpha_s$  can be determined by comparing the  $Q^2$ -dependence of the DIS cross section measurements with the predictions based on the QCD-improved parton model. In our analysis the value of  $\alpha_s$  is obtained simultaneously with the nucleon PDFs and the twist-4 terms. This allows to take into account the correlation of  $\alpha_s$  with other parameters affecting the data  $Q^2$ -dependence. The central value of  $\alpha_s$  obtained in this way depends on the perturbative order and reduces from NLO to NNLO. In particular, the ABM11 fit [4] yields

$$\begin{aligned} \alpha_s(M_Z^2) &= 0.1180 \pm 0.0012(\text{exp}) && \text{NLO}, \\ \alpha_s(M_Z^2) &= 0.1134 \pm 0.0011(\text{exp}) && \text{NNLO}. \end{aligned} \quad (2)$$

The values of  $\alpha_s$  preferred by each particular DIS data set are demonstrated in Fig. 1 by means of the  $\chi^2$ -profiles obtained in the variants of the ABM11 fit with  $\alpha_s$

<sup>c</sup>The twist-6 terms were also checked in the fit and found comparable to zero within errors applying the cut of  $Q^2 > 2.5 \text{ GeV}^2$  used in the present analysis.

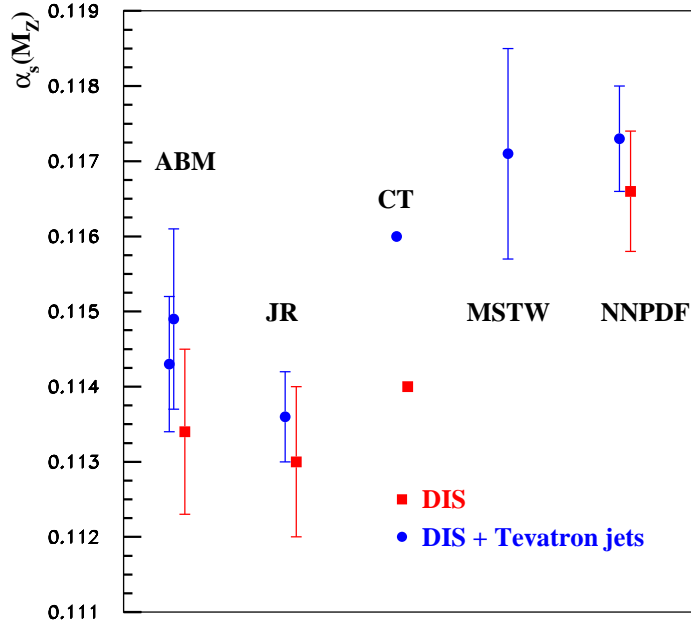


Fig. 2. The values of  $\alpha_s(M_Z^2)$  obtained in the ABM fit [4] in comparison to the ones obtained by JR [12], CTEQ [13], MSTW [14], and NNPDF [15] from the analysis of the DIS data (squares) and from the combination of the DIS and jet Tevatron data [16,17] (circles).

fixed at the values in the range of  $0.104 \div 0.130$ . The HERA and BCDMS data sets have a similar  $\chi^2$ -shape with minima around the values Eq. (2), while the SLAC and NMC data pull the value of  $\alpha_s$  somewhat up and down, respectively. Note that the two latter sets are sensitive to higher-twist terms due to substantial small- $Q^2$  contributions in these samples. In contrast, the HERA and BCDMS data are far less sensitive to higher twist terms and it is worth noting that in the variant of the ABM11 fit excluding the SLAC and NMC data and setting the higher twist terms to zero we find  $\alpha_s(M_Z^2) = 0.1133 \pm 0.0011(\text{exp.})$  at NNLO. The good agreement of this value with Eq. (2) substantiates the consistency between different data sets in our analysis once the higher twist terms are taken into account. Moreover, this cross-check confirms that the combination of the BCDMS and HERA data can be used for accurate determination of  $\alpha_s(M_Z^2)$  since these two data sets provide complimentary constraints on the PDFs [10], see also [11].

The NNLO value of  $\alpha_s$  Eq. (2) is in a good agreement with the results of the JR analysis [12] and the recent CTEQ determination [13], while the MSTW [14] and NNPDF [15] groups report substantially bigger values, cf. Fig. 2. The discrepancy with MSTW can be explained in part by impact of the jet Tevatron data, which pull

the value of  $\alpha_s(M_Z^2)$  up by  $0.001 \div 0.002$ , depending on the fit details. Furthermore, changing our fit ansatz in direction of the MSTW and NNPDF ones we approach their value of  $\alpha_s$ . In particular, dropping the higher twist terms simultaneously with an additional cut of  $W^2 > 12.5 \text{ GeV}^2$  imposed by MSTW and NNPDF we obtain  $\alpha_s(M_Z^2) = 0.1191 \pm 0.0006(\text{exp.})$ . In a similar way, disregarding the error correlation in the HERA and NMC data, like in the MSTW analysis, we obtain  $\alpha_s(M_Z^2)$  shifted by  $+0.0026$ , in the direction of the MSTW value. Note that in this context the recently updated JR analysis [12] treats the higher twist properly. The CTEQ analysis [13] seems to be less sensitive to the impact of the higher twist contributions, compared to that by MSTW and NNPDF due to a more stringent cut on  $Q^2$ .

#### 4. The Mass of the Charm Quark

The sensitivity to the charm quark mass  $m_c$  in our analysis appears essentially due to the data on the NC and CC inclusive DIS [19], and the CC semi-inclusive charm production in DIS [20, 21] with the most essential experimental constraint on  $m_c$  coming from the semi-inclusive charm-production HERA data [18]. The latter sample comprises the statistics of the H1 and ZEUS experiments obtained for different  $c$ -quark decay channels. The combination was performed similarly to the case of the inclusive HERA data [19] and allows to reduce the systematic errors of each experiment due to cross-calibration of the experiments. The FFN scheme provides a good description of the semi-inclusive HERA data up to the largest  $Q^2$ -values covered, cf. Fig. 3, with a value of  $\chi^2/NDP = 61/52$  at NNLO. Here NDP denotes the number of data points. The  $\overline{\text{MS}}$ -values of  $m_c$  found in the analysis of [22] are

$$m_c(m_c) = 1.15 \pm 0.04(\text{exp}) \begin{matrix} +0.04 \\ -0.00 \end{matrix}(\text{scale}) \quad \text{NLO}, \quad (3)$$

$$m_c(m_c) = 1.24 \pm 0.03(\text{exp}) \begin{matrix} +0.03 \\ -0.02 \end{matrix}(\text{scale}) \begin{matrix} +0.00 \\ -0.07 \end{matrix}(\text{th}), \quad \text{NNLO}_{\text{approx}}, \quad (4)$$

at NLO and NNLO, respectively, see also [23]. The experimental accuracy of 30 MeV obtained at NNLO is quite competitive with other determinations of  $m_c$  based on the  $e^+e^-$  data and the central value Eq. (4) is in a good agreement with the world average [24]. The scale error in Eqs. (3) and (4) is obtained varying the factorization scale by a factor of 1/2 and 2 around the nominal value of  $\sqrt{m_c^2 + \kappa Q^2}$ , where  $\kappa = 4$  for NC and  $\kappa = 1$  for CC heavy-quark production, respectively. In the NNLO case an additional error related to the uncertainty in the massive Wilson coefficients contributes. The value of Eq. (4) is obtained for the interpolation parameter  $d_N = -0.1$  being preferred by the fit, roughly corresponding to option A of the Wilson coefficients of Ref. [2]. Meanwhile, option B is clearly excluded by the data with  $\chi^2/NDP=115/52$ . Therefore the uncertainty due to the missing NNLO massive terms is estimated as a variation between options A and  $(A+B)/2$  which yields the value of 70 MeV Eq. (4). The value of  $m_c(m_c)$  obtained in our analysis demonstrates remarkable stability w.r.t.  $\alpha_s(M_Z^2)$ . Performing variants of our analysis with the values of  $\alpha_s$  fixed in the wide range around the best value preferred

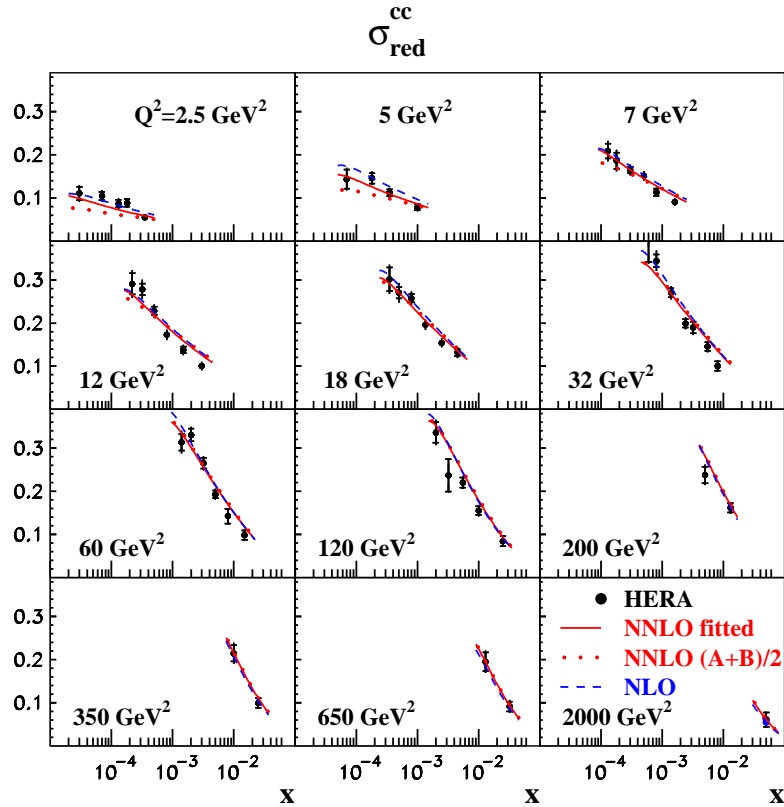


Fig. 3. The combined HERA data on the reduced cross section for the open charm production [18] versus  $x$  at different values of  $Q^2$  in comparison with the analysis of [22] at NLO (dashed line) and NNLO (solid line) together with a fit variant based on the option (A+B)/2 of the NNLO Wilson coefficients of Ref. [2], cf. Eq. (1) (dotted line); from Ref. [22].

by the data, we find a variation of  $m_c(m_c)$  in the range of 10-20 MeV, depending on the order, cf. Fig 4.

The NLO value of  $m_c(m_c)$  obtained in our analysis is somewhat lower than the one of  $m_c(m_c) = 1.26 \pm 0.05$  (exp) GeV from the analysis based on the HERA data only [18]. To understand the difference we checked the cases of a cut on  $Q^2 = 3.5$  GeV<sup>2</sup>, likewise in the HERA fit, and no semi-inclusive Tevatron data [20, 21] included. As a result we obtain shifts in  $m_c(m_c)$  by +30 MeV and +40 MeV, respectively. The remaining discrepancy should be attributed to the particularities of the HERA PDFs. The value of  $m_c(m_c)$  was recently also determined by the CTEQ collaboration [25]. In contrast to our case this determination is based on the S-ACOT- $\chi$  prescription as GMVFN scheme. Furthermore, the  $\overline{\text{MS}}$  coefficients of Ref. [25] are obtained by straightforward substitution of the pole- and running-mass matching relation into the pole-mass coefficients. The expressions obtained in such

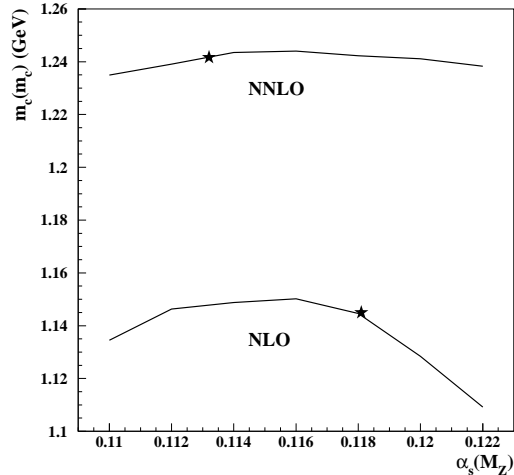


Fig. 4. The values of  $m_c(m_c)$  obtained in the NLO and NNLO variants of our analysis with the value of  $\alpha_s(M_Z^2)$  fixed. The position of the star displays the result with the value of  $\alpha_s(M_Z^2)$  fitted [4]; from Ref. [22].

a way correspond to a mixed order in  $\alpha_s$ . Moreover, the advantage of this approach is not evident in view of the poor perturbative convergence of the mass matching relation. The central CTEQ value of  $m_c(m_c) = 1.12^{+0.11}_{-0.17}$  GeV is lower than the world average, while the CTEQ errors are much larger than those in Eqs. (3) and (4) due to the impact of the uncertainty in the GMVFN scheme modeling.

## 5. VFN Uncertainties

The choice of the factorization scheme plays an essential role in the analysis of existing DIS data due to important constraints coming from the small- $x$  region, where the heavy quark contribution is numerically large. While our analysis is based on the FFN scheme, many other groups employ different variants of the GMVFN scheme, which differ by *modeling* of the low- $Q^2$  region. The spread between these variants is rather substantial and thus implies a corresponding uncertainty in the basic parameters determined in these GMVFN fits. In particular, the value of  $m_c$  determined from a combination of the inclusive and semi-inclusive HERA data with the different versions of the ACOT and RT prescriptions for the VFN scheme demonstrate a spread of 400 MeV [18]. There are also sources of the VFN scheme uncertainties, which are common for all these prescriptions. Firstly, the matching of heavy-quark PDFs is commonly performed at the factorization scale  $\mu$  equal to the  $\mu_0 = m_c$ , resp.  $m_b$ . Clearly, at these scales neither of the heavy flavors can be dealt with as massless. The matching point  $\mu_0$  is not fixed by theory and in principle it can vary in a wide range being an artefact of the description not



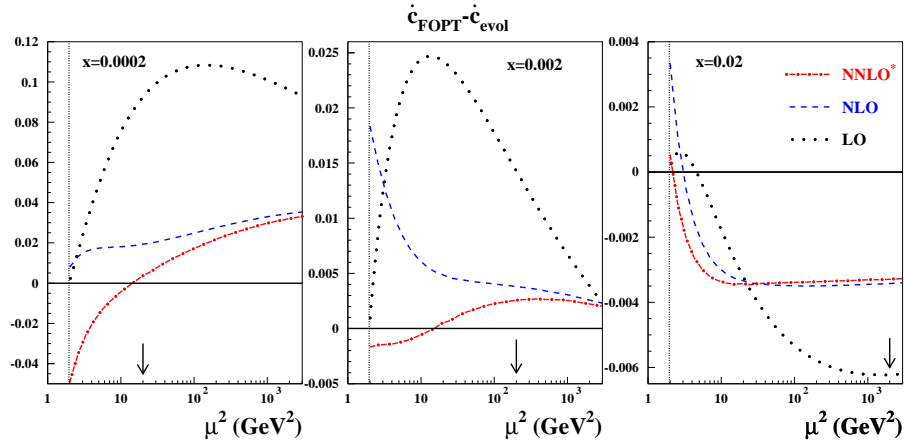


Fig. 5. The difference between the  $c$ -quark PDFs derivatives  $\dot{c}(x, \mu^2) \equiv \frac{dc(x, \mu^2)}{d \ln \mu^2}$  calculated with the FOPT matching condition and with the massless 4-flavor evolution starting at the matching point  $\mu_0 = m_c = 1.4$  GeV versus the factorization scale  $\mu^2$  at different values of  $x$  in the LO, NLO, and NNLO\* approximations. The arrows display upper margin of the HERA collider kinematics with the collision c.m.s. energy squared  $s = 10^5$  GeV<sup>2</sup> and the vertical lines correspond to the matching point position  $\mu_0$ .

contributing to the observables according to the renormalization group equations. Additional uncertainty emerge for the 4(5)-flavor PDFs in the NNLO analysis. They are commonly matched with the 3(4)-flavor ones using *NLO matching condition*, since the NNLO OMEs are not yet known in the complete form<sup>d</sup>. However, to provide consistency with the NNLO Wilson coefficients the evolution of these PDFs is performed in the NNLO approximation that introduces an additional uncertainty due to missing higher-order corrections into the analysis. At the same time, the evolution of the 4(5)-flavor PDFs in the VFN scheme leads to a resummation of the terms  $\sim \ln(\mu^2)$  which in part reproduce the higher-order corrections, being known, however, not to be dominant. Relations between the resummation effects and the VFN evolution uncertainties are illustrated in Fig. 5 by comparison of the  $\mu$ -derivatives for the  $c$ -quark distribution being calculated in different ways. In one case the distributions are matched at the scale of  $\mu_0$  using the fixed-order-perturbation-theory (FOPT) matching conditions and then evolved starting from  $\mu_0$  with the massless splitting functions. In another case they are calculated with the FOPT matching conditions at all scales. The difference between these two cases do not demonstrate a significant rise with  $\mu$ . The only exclusion is observed at  $x \lesssim 0.0001$  and at scales outside of the kinematics being probed in experiment. Therefore it cannot be attributed to the impact of the log-term resummation. In contrast, there is a substantial difference in the derivatives calculated in the NLO

<sup>d</sup> For progress in this field cf. [26–29].

and NNLO\*, i.e. the combination of the NLO matching with the NNLO evolution. This difference yields an estimate of the uncertainty in the VFN scheme due to the missing higher-orders, which is obviously larger than the resummation effects. Checking the impact of this uncertainty w.r.t. the value of  $\alpha_s(M_Z^2)$  in combination with the variation of the matching point for the 4-flavor PDFs in the range of  $1.2 \div 1.5$  GeV we find a value of  $\pm 0.001$ . This is comparable to the experimental uncertainty and makes the VFN schemes incompetent with the FFN one in the precision determination of  $\alpha_s(M_Z^2)$ .

### Acknowledgments

We thank P. Jimenez-Delgado and E. Reya for discussions. This work has been supported in part by Helmholtz Gemeinschaft under contract VH-HA-101 (*Alliance Physics at the Terascale*), DFG Sonderforschungsbereich/Transregio 9 and by the European Commission through contract PITN-GA-2010-264564 (*LHCPhenoNet*).

### References

1. S. Bethke *et al.*, *Workshop on Precision Measurements of  $\alpha_s$* , arXiv:1110.0016 [hep-ph].
2. H. Kawamura, N. A. Lo Presti, S. Moch and A. Vogt, *Nucl. Phys. B* **864**, 399 (2012).
3. S. Alekhin and S. Moch, *Phys. Lett. B* **699**, 345 (2011).
4. S. Alekhin, J. Blümlein and S. Moch, *Phys. Rev. D* **86**, 054009 (2012);
5. S. Catani, M. Ciafaloni and F. Hautmann, *Nucl. Phys. B* **366**, 135 (1991).
6. I. Bierenbaum, J. Blümlein and S. Klein, *Nucl. Phys. B* **820**, 417 (2009).
7. T. Gottschalk, *Phys. Rev. D* **23**, 56 (1981).
8. M. Glück, S. Kretzer and E. Reya, *Phys. Lett. B* **380**, 171 (1996) [Erratum-ibid. B **405**, 391 (1997)].
9. J. Blümlein, A. Hasselhuhn, P. Kovacikova and S. Moch, *Phys. Lett. B* **700** 294 (2011).
10. C. Adloff *et al.* [H1 Collaboration], *Eur. Phys. J. C* **21**, 33 (2001).
11. S. Alekhin, J. Blümlein and S. Moch, arXiv:1303.1073 [hep-ph].
12. P. Jimenez-Delgado and E. Reya, private communication.
13. J. Gao *et al.*, arXiv:1302.6246 [hep-ph].
14. A. Martin, W. J. Stirling, R. Thorne and G. Watt, *Eur. Phys. J. C* **64**, 653 (2009).
15. R. D. Ball *et al.*, *Phys. Lett. B* **707**, 66 (2012).
16. A. Abulencia, *et al.*, *Phys. Rev. D* **75**, 092006 (2007).
17. V. Abazov, *et al.*, *Phys. Rev. Lett.* **101**, 062001 (2008).
18. H. Abramowicz *et al.* [H1 and ZEUS Collaborations], *Eur. Phys. J. C* **73**, 2311 (2013).
19. F. D. Aaron *et al.* [H1 and ZEUS Collaboration], *JHEP* **1001**, 109 (2010).
20. A. O. Bazarko *et al.* [CCFR Collaboration], *Z. Phys. C* **65**, 189 (1995).
21. M. Goncharov *et al.* [NuTeV Collaboration], *Phys. Rev. D* **64**, 112006 (2001).
22. S. Alekhin *et al.*, *Phys. Lett. B* **720** (2013) 172
23. S. Alekhin, K. Daum, K. Lipka and S. Moch, *Phys. Lett. B* **718** (2012) 550
24. J. Beringer *et al.* [Particle Data Group Collaboration], *Phys. Rev. D* **86**, 010001 (2012).
25. J. Gao, M. Guzzi and P. M. Nadolsky, arXiv:1304.3494 [hep-ph].
26. J. Ablinger *et al.*, *PoS LL* **2012** (2012) 033.
27. J. Ablinger *et al.*, *Nucl. Phys. B* **864** (2012) 52.
28. J. Ablinger *et al.*, *Nucl. Phys. B* **844** (2011) 26.
29. J. Blümlein, A. Hasselhuhn, S. Klein and C. Schneider, *Nucl. Phys. B* **866** (2013) 196.

